Drug Development and Industrial Pharmacy

ISSN: 0363-9045 (Print) 1520-5762 (Online) Journal homepage: www.tandfonline.com/journals/iddi20

Preclinical evaluation of *Asparagus stipularis* in a rat model of metabolic syndrome and development of its nanoencapsulated form

Khaoula Adouni , Olfa Zouaoui , Pedro Brandão , Patrícia Rijo , Sofia A. Costa Lima , Salette Reis , Lotfi Achour & Pedro Fonte

To cite this article: Khaoula Adouni , Olfa Zouaoui , Pedro Brandão , Patrícia Rijo , Sofia A. Costa Lima , Salette Reis , Lotfi Achour & Pedro Fonte (2026) Preclinical evaluation of *Asparagus stipularis* in a rat model of metabolic syndrome and development of its nanoencapsulated form, Drug Development and Industrial Pharmacy, 52:7, 1377-1390, DOI: 10.1080/03639045.2026.2674218

To link to this article: https://doi.org/10.1080/03639045.2026.2674218

Published online: 02 Jun 2026.

DRUG DEVELOPMENT AND INDUSTRIAL PHARMACY
2026, VOL. 52, NO. 7, 1377–1390
https://doi.org/10.1080/03639045.2026.2674218

Taylor & Francis
by informa

RESEARCH ARTICLE

Preclinical evaluation of *Asparagus stipularis* in a rat model of metabolic syndrome and development of its nanoencapsulated form

Khaoula Adouni[a], Olfa Zouaoui[a], Pedro Brandão[b,c,d,e], Patrícia Rijo[f,g], Sofia A. Costa Lima[h,*], Salette Reis[h], Lotfi Achour[a] and Pedro Fonte[c,d,i,j]

[a]Laboratoire de Recherche "Bioressources: Biologie Intégrative & Valorisation", Institut Supérieur de Biotechnologie de Monastir, Université de Monastir, Monastir, Tunisia; [b]Egas Moniz School of Health & Science, Egas Moniz Center for Interdisciplinary Research (CiiEM), Caparica, Almada, Portugal; [c]Department of Bioengineering, iBB-Institute for Bioengineering and Biosciences, Instituto Superior Técnico, Universidade de Lisboa, Lisbon, Portugal; [d]Associate Laboratory i4HB – Institute for Health and Bioeconomy at Instituto Superior Técnico, Universidade de Lisboa, Lisbon, Portugal; [e]Department of Chemistry, CQC-IMS, University of Coimbra, Coimbra, Portugal; [f]CBIOS – Research Center for Biosciences & Health Technologies, Universidade Lusófona de Humanidades e Tecnologias, Lisbon, Portugal; [g]Faculty of Pharmacy, Research Institute for Medicines (iMed.ULisboa), Universidade de Lisboa, Lisbon, Portugal; [h]Department of Chemical Sciences – Applied Chemistry Lab, Faculty of Pharmacy, LAQV, REQUIMTE, University of Porto, Porto, Portugal; [i]Centro de Ciências do Mar do Algarve (CCMAR/CIMAR LA), Universidade do Algarve, Faro, Portugal; [j]Department of Chemistry and Pharmacy, Faculty of Sciences and Technology, University of Algarve, Faro, Portugal

ABSTRACT

Context: Asparagus stipularis Forssk decoction (ASD) has shown potential metabolic and antioxidant benefits, yet its effects on pancreatic dysfunction associated with metabolic syndrome remain insufficiently explored.

Objective: The aim of this work was to assess the pancreatic protective properties of ASD in high-fructose diet (HFrD)-fed rats and to characterize ASD-loaded poly(lactic-co-glycolic acid) (PLGA) nanoparticles (NPs) as a delivery system to enhance its therapeutic potential.

Methods: Rats were fed an HFrD and treated with ASD at two dose levels. Serum α-amylase and lipase activities were measured to assess digestive enzyme modulation. Pancreatic lipid peroxidation was quantified using thiobarbituric acid reactive substances (TBARS), while antioxidant enzyme activities, including superoxide dismutase, catalase, and glutathione peroxidase, were determined. Histopathological examination was performed to evaluate structural alterations in pancreatic tissues. ASD was encapsulated into PLGA NPs, and particle size, polydispersity index (PdI), zeta potential (ZP), and encapsulation efficiency (EE) were analyzed.

Results: ASD significantly reduced serum α-amylase activity to 2285.3 ± 256.6 U/L (low dose) and 1846.4 ± 82.8 U/L (high dose) compared to HFrD controls. Serum lipase activity decreased by 13% and 18% at the respective doses. TBARS levels were markedly reduced, and antioxidant enzyme activities were restored to near-control levels. Histological analysis revealed improved β-cell morphology and reduced acinar degeneration. ASD-loaded PLGA NPs exhibited a mean size of 248 ± 5 nm, PdI of 0.13 ± 0.01, ZP of −24.7 ± 1.3 mV, and an EE of 75.5 ± 3.2%.

Conclusion: ASD demonstrates significant pancreatic protective effects, and nanoencapsulation enhances its therapeutic promise for metabolic disorders.

ARTICLE HISTORY
Received 26 July 2025
Revised 26 March 2026
Accepted 9 May 2026

KEYWORDS
Asparagus stipularis; α-amylase; pancreatic lipase; high-fructose diet; oxidative stress; PLGA nanoparticles

Introduction

The global prevalence of type 2 diabetes mellitus (T2DM) has increased dramatically in recent decades, representing a major global health concern. The International Diabetes Federation [1] estimates that about 589 million adults aged 20–79 years are currently affected, corresponding to 11.1% of the global population. Likewise, the World Health Organization [2] reported in 2022 that approximately 14% of adults aged 18 years and older have diabetes – more than twice the prevalence observed in 1990. This upward trend is strongly associated with modern dietary habits, particularly the high intake of fructose from table sugar, high-fructose corn syrup, soft drinks, and processed foods. Excessive fructose consumption induces profound metabolic disturbances, such as impaired glucose tolerance, dyslipidemia, and hypertension, largely through its lipogenic action and effects on

CONTACT Pedro Fonte prfonte@ualg.pt Department of Chemistry and Pharmacy, Faculty of Sciences and Technology, University of Algarve, Faro, Portugal
*LAQV, REQUIMTE, Instituto de Ciências Biomédicas Abel Salazar, Rua de Jorge Viterbo Ferreira, 228, Porto, 4050-313, Portugal.

pancreatic β-cell function [3–5]. Chronic exposure to fructose promotes β-cell overstimulation, oxidative stress, and islet damage, leading to insulin secretion impairment and features of metabolic syndrome [6,7]. Current pharmacological interventions, including insulin therapy and oral antidiabetic drugs, often have limitations such as hypoglycemic episodes, fat accumulation, and limited efficacy against diabetes-associated complications [8]. Moreover, achieving stable and bioavailable delivery of therapeutic proteins remains challenging [9]. In this context, natural products are being increasingly explored as alternative antidiabetic agents. Medicinal plants, rich in antioxidants and bioactive phytochemicals, can modulate glucose metabolism, promote β-cell regeneration, and enhance insulin activity [10–12]. Among these, species of *Asparagus* – notably *Asparagus stipularis Forssk.* – are traditionally used in folk medicine for diabetes management. Previous studies, including our own, demonstrated that *A. stipularis* extract lowers blood glucose and mitigates oxidative stress in rats fed a high-fructose diet (HFrD) [13]. Nevertheless, the therapeutic potential of plant extracts is limited by the instability and poor bioavailability of their active constituents. Encapsulation within polymeric nanocarriers such as poly(lactic-co-glycolic acid) (PLGA) nanoparticles (NPs) may enhance stability, bioavailability, and sustained release of these bioactives [14–16]. Despite the extensive use of PLGA systems in drug delivery, no study has yet examined the protective effects of *A. stipularis* on pancreatic tissue *in vivo*, neither the compatibility and encapsulation efficiency (EE) of this extract into a nanoformulation was evaluated thus far. Therefore, the present work aimed to assess the effects of *A. stipularis* shoot decoction on carbohydrate and lipid metabolism, oxidative stress, and pancreatic histopathology in rats fed a HFrD, and to develop a PLGA NP formulation encapsulating this decoction, in order to evaluate its physicochemical properties and its feasibility to be further studied in the future for its health benefits. This integrated pharmacological and nanotechnological approach may offer a novel strategy for the development of plant-based therapies for T2DM.

Materials and methods

Plant material

Shoots of *A. stipularis* were collected in January (2015) from the cliff of Monastir (Tunisia). The plant material was dried by active ventilation and later ground in an ultra-centrifugal mill ZM 200 (Retsch, Haan, Germany). The plant was identified by Pr. Fethia Harzallah Skhiri, a qualified botanist at the Higher Institute of Biotechnology of Monastir, Tunisia. As the plant was identified specifically for this research and not deposited in a formal herbarium, no voucher/approval number was assigned.

Preparation of decoction

Dry shoots (10 g) were added to 2 L of distilled water and boiled for 5 min [13]. The mixture was cooled and filtered under reduced pressure. The obtained decoction was frozen before being lyophilized (FreeZone 4.5, Labconco, Kansas City, MO) and the dry extract was designed as ASD (*Asparagus* shoots decoction).

Animals, diet, and experimental study design

Male Wistar rats aged 8–10 weeks, weighing 180–200 g, were used in the experimental investigation of this study. The experimental protocol was approved by the National Ethics Committee ENMV under authorization numbers ECM 3129/24 and CER 0017/2026-0211, in accordance with the US National Institutes of Health guidelines (NIH No. 85-23, revised 1996) and approval number ECM#2024-3129. The rats were housed in cages in the Central Animal House and fed standard pellet diet and tap water. The rats were divided into seven groups, with each containing eight rats and treated as described below:

- *Group* 1 *(normal control)*: Rats fed a standard chow and drinking water for 5 months.
- *Group* 2 *(HFrD)*: Rats fed a HFrD (10% fructose solution) instead of water for 5 months as the negative control.
- *Group* 3 *(HFrD + Met)*: Rats fed a HFrD for 5 months and administered with metformin (150 mg/kg, orally, once daily in the morning) for the last 4 weeks as the positive control.
- *Group* 4 *(HFrD + ASD (L))*: Rats fed a HFrD for 5 months and administered ASD (100 mg/kg, orally, once daily in the morning) for the last 4 weeks.
- *Group* 5 *(HFrD + ASD (H))*: Rats fed a HFrD for 5 months and administered ASD (300 mg/kg, orally, once daily in the morning) for the last 4 weeks.
- *Group* 6 *(Cont + ASD (L))*: Rats fed with a standard chow and drinking water for 5 months and administered ASD (100 mg/kg, orally, once daily in the morning) for the last 4 weeks.
- *Group* 7 *(Cont + ASD (H))*: Rats fed with a standard chow and drinking water for 5 months and administered ASD (300 mg/kg, orally, once daily in the morning) for the last 4 weeks.

Effects of A. stipularis on α-amylase and pancreatic lipase activities

At the end of experimental period, the animals were anesthetized by inhalation of diethyl ether. Blood samples were obtained from cardiac puncture in an empty vacutainer tube and centrifuged at 4000 × *g* for 10 min at 4 °C. Plasma was then collected and α-amylase and pancreatic lipase were analyzed with an automatic analyzer (Roche Diagnostics, Mannheim, Germany). Enzyme activity results were then expressed as U/L.

Pancreatic markers of oxidative stress

Following blood collection, an abdominal incision was made, and the pancreas was removed and immediately washed with ice-cold physiologic saline solution (0.9%, w/v), blotted dry and weighed. About 0.4 g of the pancreas was cut into small pieces, homogenized in 3 mL ice-cold appropriate buffer (TBS, pH 7.4) using an Ultra Turrax homogenizer T25 (Cole-Parmer, Vernon Hills, IL) and then centrifuged at 9000 × *g* for 15 min at 4 °C. Supernatants were collected, aliquoted, and kept at −80 °C until use for enzyme assays. The total protein content in each sample was determined using the Bradford method, which relies on protein–dye binding and provides rapid and sensitive quantitation of microgram protein levels [17].

Measurement of lipid peroxidation products

Lipid peroxidation (LP) was assessed by measuring thiobarbituric acid reactive substances (TBARS), including malondialdehyde (MDA). In an acidic and hot medium, one molecule of MDA condenses with two molecules of thiobarbituric acid (TBA) to form a pink-colored complex that can be detected at 530 nm. Briefly, 125 µL of supernatant was mixed with 150 µL of trichloroacetic acid (TCA, 40%), stirred, and centrifuged at 3000 rpm for 10 min. Subsequently, 200 µL of the resulting supernatant was combined with 160 µL of TBA (120 mM), mixed, and incubated at 80 °C for 15 min. The absorbance was measured at 530 nm and was proportional to the amount of TBARS formed [18,19].

Assay for antioxidative status in pancreas homogenate

Catalase activity

Catalase (CAT) activity was determined by measuring the rate of hydrogen peroxide (H_2O_2) decomposition according to the method described by Nasri et al. [18]. The reaction mixture consisted of 780 µL of phosphate buffer (100 mM, pH 7.0), 200 µL of freshly prepared H_2O_2 (500 mM), and 20 µL of tissue supernatant. The decrease in absorbance was kinetically monitored at 240 nm for 1 min. Enzyme activity was calculated using an H_2O_2 extinction coefficient of 0.043 mM^{-1} cm^{-1}, and the results were expressed as units per milligram of protein (U/mg protein).

Superoxide dismutase activity

Superoxide dismutase (SOD) activity was determined according to the method previously described by Nasri et al. [18]. Briefly, 1000 µL of EDTA (2.69 mM)–methionine (39 mM) solution was added to 892.2 µL of phosphate buffer (TPO_4, 50 mM, pH 7.8), followed by 50 µL of tissue supernatant, 950 µL of phosphate buffer, 85.2 µL of nitro blue tetrazolium (NBT, 1 mM), and 22.6 µL of riboflavin (1 mM). The mixture was incubated under white light for 20 min. Two additional tubes were prepared: the first served as a blank (kept in the dark for spectrophotometer zeroing), and the second was used for total activity measurement, incubated under light under the same conditions as the samples. The optical density was read at 580 nm. One unit of SOD activity was defined as the amount of enzyme required to inhibit 50% of NBT oxidation, and the results were expressed as U/mg protein.

Glutathione peroxidase activity

Glutathione peroxidase (GPx) activity was determined according to the method described by Histo Flohé and Günzler [20], H_2O_2 was used as the substrate. GPx activity was calculated based on the decrease in reduced glutathione (GSH) levels relative to the non-enzymatic reaction. For the enzymatic assay, 0.2 mL of tissue supernatant was mixed with 0.4 mL of reduced GSH (1 mM) and 0.2 mL of Tris-buffered saline (TBS; pH 7.8). The mixture was incubated at 25 °C for 5 min, followed by the addition of 0.2 mL of H_2O_2 (1.3 mM) to initiate the reaction. After 10 min, the reaction was terminated by adding 1 mL of TCA (1%) and placing the tubes on ice for 30 min. The samples were then centrifuged at 3000 rpm for 10 min. Subsequently, 0.48 mL of the supernatant was added to 2.2 mL of sodium phosphate buffer (Na_2HPO_4; 0.32 M) and 0.32 mL of 5,5′-dithio-bis(2-nitrobenzoic acid) (DTNB; 1 mM). Absorbance was measured at 412 nm within 5 min. For the non-enzymatic control, the same reagents were used without the tissue supernatant. GPx activity was expressed as U/mg protein.

Histopathological examination

A small portion of the pancreas was sampled and immediately fixed in Bouin's solution for at least 48 h. Following fixation, tissues were processed using a graded ethanol series for dehydration: 70%, 80%, 95%, and 100% ethanol, each for 1–2 h. This was followed by clearing in xylene and infiltration with molten paraffin wax at 60 °C. Tissues were embedded in paraffin blocks and sectioned at 5 µm thickness using a rotary microtome. Sections were mounted on glass slides, deparaffinized in xylene, rehydrated through a descending ethanol series, and stained with hematoxylin and eosin (H&E) for histopathological examination under an Olympus CX41 light microscope (Hachioji, Japan) [21].

Extract encapsulation into nanoparticles

ASD-loaded PLGA nanoparticles

To produce PLGA NPs, a modified solvent emulsification–evaporation method was adopted as previously described by Fonte et al. [22]. PLGA 50:50 (100 mg) was dissolved in dichloromethane (2 mL) to create an organic phase. After that, 0.2 mL of ASD were added and the mixture was sonicated for 30 s at 70% amplitude using a Q125 Sonicator (QSonica Sonicators, Newtown, CT). Then, the emulsion was quickly added to PVA (10 mL, 2% w/v) and sonicated under the same conditions. To evaporate the organic solvent, the emulsion was magnetically stirred for 3 h at room temperature. Unloaded PLGA NPs were elaborated following the same procedure and used as control.

Physicochemical properties of nanoparticles

Particle size, polydispersity index (PdI), and zeta potential (ZP) of the ASD-loaded NPs were analyzed using a Coulter Nano-sizer Delsa™ Nano C from Beckman Coulter, Inc. (Brea, CA). The samples were diluted with distilled water. The mean particle size and PdI of NPs were analyzed by dynamic light scattering (DLS). Electrophoretic mobility analysis was used to calculate the ZP. Experiments were carried out in triplicate.

Determination of encapsulation efficiency

The EE of the ASD loaded into PLGA NPs was measured using total phenolic content (TPC) analysis as previously described by our group, since *A. stipularis* presents several phenolic compounds, namely hydroxycinnamoyl derivatives such as caffeic acid [23]. By measuring the amount of unloaded free TPC in the supernatant recovered after centrifuging the NP suspension at 15,000 rpm for 20 min, the quantity of TPC entrapped within the NPs was determined. The NPs were centrifuged, re-suspended in bidistilled water, and then freeze-dried for 48 h at −50 °C and 400 mTorr using a LABCONCO FreeZone 25® freeze dryer (Kansas City, MO). The TPC was determined by ultraviolet–visible (UV–vis) spectrophotometry at 765 nm. EE was calculated according to the formula:

$$EE\,\% = \frac{\text{amount of TPC in the encapsulated extract} - \text{amount of TPC in the supernatant}}{\text{amount of TPC in the encapsulated extract}} \times 100$$

Scanning electron microscopy (SEM) analysis

A FEI Quanta 400 FEG SEM (FEI, Hillsboro, OR) was used to study the morphology of NPs. The nanocarrier samples were placed on metal stubs, and vacuum-coated with a layer of gold/palladium for 60 s with a current of 15 mA, prior to observation in the equipment.

Fourier transform infrared (FTIR) spectroscopic analysis

ATR-FTIR was used to characterize the molecular composition of the ASD, PLGA, the physical mixture (shoots decoction and PLGA), and unloaded and loaded PLGA NPs. The analysis was carried out using a MB3000 FTIR spectrometer (ABB, Zurich, Switzerland) linked to a MIRacle single reflection attenuated total reflectance (ATR) accessory from PIKE Technologies (Madison, WI). All spectra were registered between 600 and 4000 cm^{-1} with 50 scans at a resolution of 4 cm^{-1}.

Differential scanning calorimetry analysis

An analysis was performed using a differential scanning calorimetry (DSC) device 200 F3 Maia (Netzsch, Selb, Germany) on the shoots decoction, PLGA, physical mixture (shoots decoction and PLGA), and unloaded and loaded PLGA NPs. Each sample (2 mg) was sealed in an aluminum pan. With a heating rate of 10 °C/min from 20 °C to 260 °C, the heating curves were recorded. An empty pan was used as reference.

Statistical analyses

Data are presented as mean ± standard error (SE). Statistical analyses were performed using SPSS version 18.0 (Statistical Package for Social Sciences, Chicago, IL). Comparisons between groups were conducted using one-way ANOVA, followed by Duncan's multiple range test. A value of $p < 0.05$ was considered statistically significant.

Results

In vivo inhibition assay of α-amylase

Compared to the control group, the serum α-amylase activity showed a significant augmentation in HFrD group, where it raised up to 3376.6 ± 384.9 U/L (Figure 1). However, the ASD administration to HFrD rats significantly lowered the serum α-amylase activity, reaching 2285.3 ± 256.6 and 1846.4 ± 82.8 U/L ($p < 0.05$) for HFrD + ASD (L) and HFrD + ASD (H), respectively. In the Cont + ASD groups, rats exhibited α-amylase activity similar to the control group. It is worthy to note that ASD effect was almost equal to that showed by metformin.

In vivo inhibition assay of pancreatic lipase

The lipase activities in all experimental rat groups were determined (Figure 2). The findings of the present study demonstrated that, when compared to the control rats, HFrD increased lipase activity (70.46 ± 0.33 U/L) as expected. However, after the administration of ASD to rats, a considerable reduction in serum lipase activity by 18% and 13% was observed in HFrD + ASD (H) and HFrD + ASD (L), respectively. Lipase activities in Cont, Cont + ASD (H), and Cont + ASD (L) rat groups were similar ($p > 0.05$).

Pancreatic TBARS

In the present study, the LP markers measured as TBARS were significantly ($p < 0.05$) increased in HFrD group (0.91 ± 0.06 nmol/mg pt) when compared with the control group (0.50 ± 0.07 nmol/mg pt) (Figure 3). However, a significant ($p < 0.05$) decrease in pancreatic TBARS levels was observed after the oral administration of ASD and metformin compared to the HFrD group.

Effect of ASD on enzymatic antioxidants

Table 1 describes the activities of enzymatic antioxidants such as CAT, SOD, and GPx in pancreatic tissues of control and experimental groups of rats. The activities were significantly reduced ($p < 0.05$) in the pancreatic tissues of the HFrD group of rats compared to control for GPx (50%), SOD (47.09%), and CAT (51.46%). Administration of ASD for HFrD groups completely

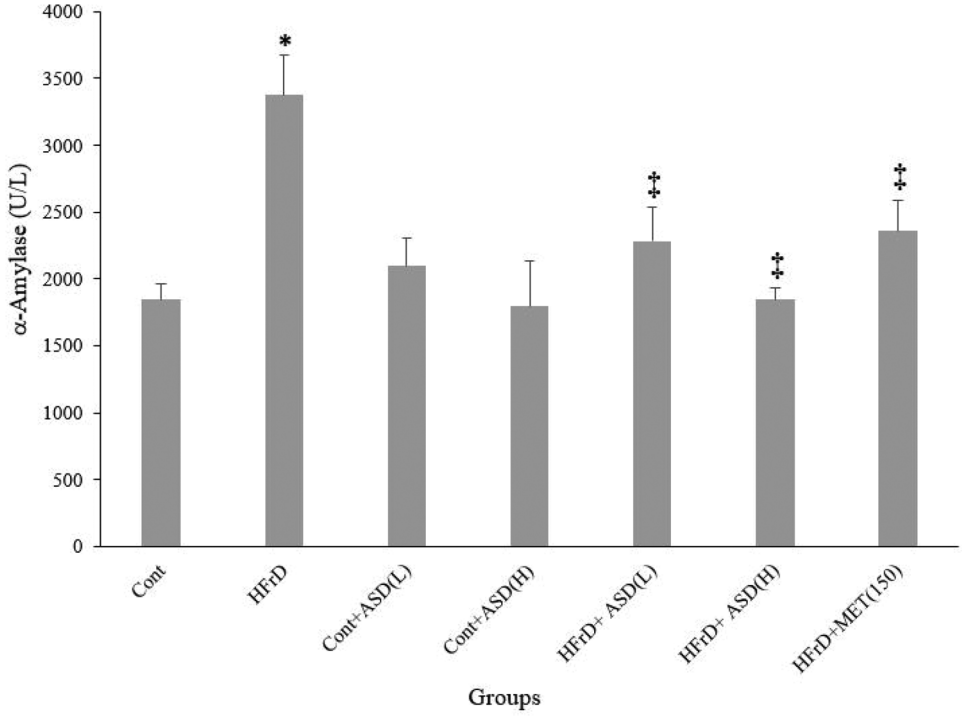

Figure 1. Effect of ASD on α-amylase activity. Cont: normal diet; HFrD: HFrD (10% fructose); Cont + ASD (L): normal diet + ASD (100 mg/kg bw); Cont + ASD (H): normal diet + ASD (300 mg/kg bw); HFrD + ASD(L): HFrD (10% fructose) + ASD (100 mg/kg bw); HFrD + ASD (H): HFrD (10% fructose) + ASD (300 mg/kg bw); HFrD + Met: HFrD (10% fructose) + metformin (150 mg/kg bw). Values are means ± SD of eight rats in each group. *A significant difference ($p < 0.05$) compared with the normal group. ‡A significant difference ($p < 0.05$) compared with the HFrD group.

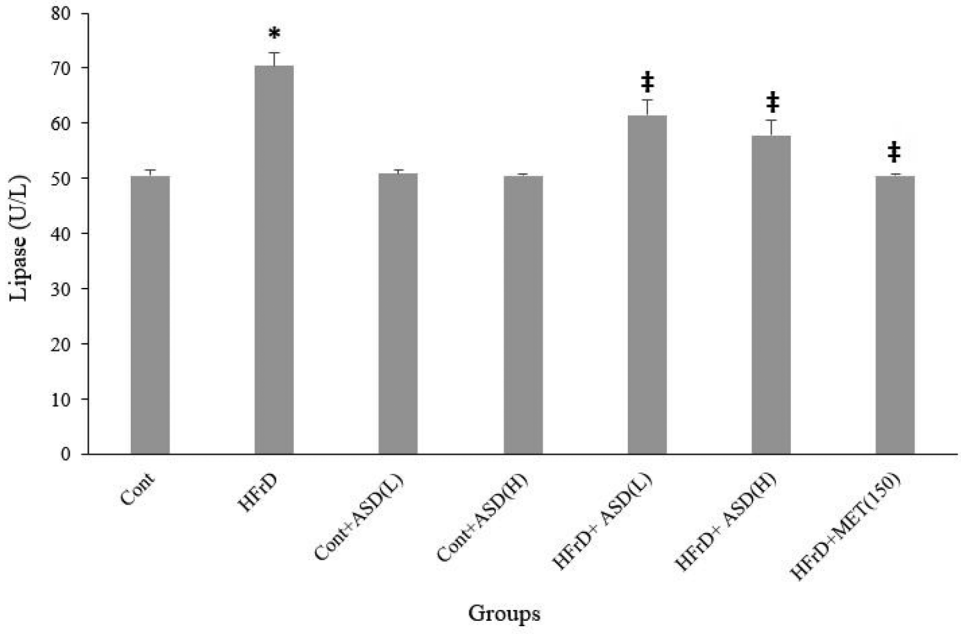

Figure 2. Effect of ASD on lipase activity. Cont: normal diet; HFrD: HFrD (10% fructose); Cont + ASD (L): normal diet + ASD (100 mg/kg bw); Cont + ASD (H): normal diet + ASD (300 mg/kg bw); HFrD + ASD(L): HFrD (10% fructose) + ASD (100 mg/kg bw); HFrD + ASD (H): HFrD (10% fructose) + ASD (300 mg/kg bw); HFrD + Met: HFrD (10% fructose) + metformin (150 mg/kg bw). Values are means ± SD of eight rats in each group. *A significant difference ($p < 0.05$) compared with the normal group. ‡A significant difference ($p < 0.05$) compared with the HFrD group.

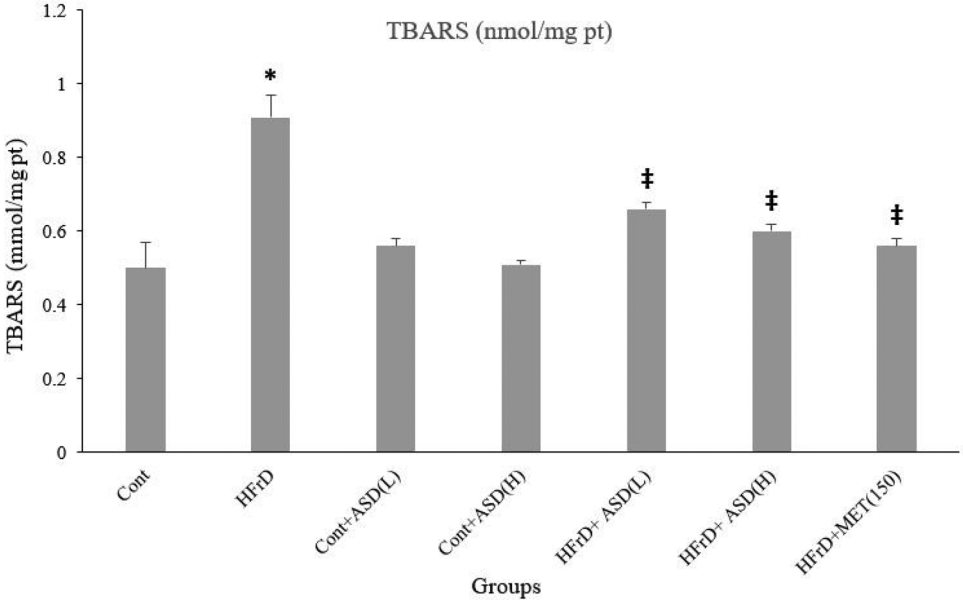

Figure 3. Effects of the ASD extract on pancreatic TBARS (Cont: normal diet; HFrD: HFrD (10% fructose); Cont + ASD (L): normal diet + ASD (100 mg/kg bw); Cont + ASD (H): normal diet + ASD (300 mg/kg bw); HFrD + ASD(L): HFrD (10% fructose) + ASD (100 mg/kg bw); HFrD + ASD (H): HFrD (10% fructose) + ASD (300 mg/kg bw); HFrD + Met: HFrD (10% fructose) + metformin (150 mg/kg bw)). Values are means ± SD of eight rats in each group. *A significant difference ($p < 0.05$) compared with the normal control group. ‡A significant difference ($p < 0.05$) compared with the HFrD group.

prevented HFrD induced decrease in the activities of these enzymes in the pancreas. The protective effect of ASD at 300 mg/kg was comparable to that of the metformin-treated group in this study.

Histopathology study

Histopathological examination of pancreatic tissues from all experimental groups is illustrated in Figure 4. Normal pancreatic architectures, including the normal acinar cell

Table 1. Effects of the ASD extract on pancreatic enzymatic antioxidants.

	SOD	CAT	GPx
Cont	112.20 ± 2.00	15.04 ± 1.01	1.14 ± 0.10
Cont + ASD (L)	110.29 ± 1.09	14.15 ± 0.20	1.03 ± 0.12
Cont + ASD (H)	105.10 ± 3.80	15.25 ± 0.90	1.21 ± 0.03
HFrD	59. 36 ± 2.10*	7. 30 ± 1.08*	0.57 ± 0.08*
HFrD + ASD (L)	60.75 ± 1.27	10.10 ± 0.60‡	0.69 ± 0.05
HFrD + ASD (H)	88.69 ± 3.70‡	13.40 ± 1.40‡	0.86 ± 0.02‡
HFrD + Met	90.24 ± 1.10‡	14.89 ± 0.80‡	0.90 ± 0.03‡

Cont: normal diet; HFrD: HFrD (10% fructose); Cont + ASD (L): normal diet + ASD (100 mg/kg bw); Cont + ASD (H): normal diet + ASD (300 mg/kg bw); HFrD + ASD (L): HFrD (10% fructose) + ASD (100 mg/kg bw); HFrD + ASD (H): HFrD (10% fructose) + ASD (300 mg/kg bw); HFrD + Met: HFrD (10% fructose) + metformin (150 mg/kg bw). Values are means ± SD of eight rats in each group.
*A significant difference ($p < 0.05$) compared with the normal control group.
‡A significant difference ($p < 0.05$) compared with the HFrD group).

and normal cells of pancreatic Langerhans islets, were seen in the control group (Figure 4(A,B), ×40). Likewise, ASD treatment of rats supplied with the control diet (Figure 4(C,D), ×40) had no significant effect, with pancreas sections appearing normal without inflammatory cell collections or other changes, ensuring the absence of toxicity of this extract at the administrated doses toward acinar and endocrine cells. The morphology was however altered on the HFrD rats' group as depicted by a severe β-cells atrophy as well as fatty deposition in acinar cells (Figure 4(E), ×40), acinar cell degeneration and fibrosis (Figure 4(F), ×40). Treatment with metformin led to a partial regeneration of islets of Langerhans (Figure 4(G,H)× 40). An alleviation in the histopathological changes of the pancreas was noted in HFrD rats exposed to ASD (L) (Figure 4(I), ×10, Figure 4(J), ×40) and ASD (H) (Figure 4(K,L), ×40) with the high dose treated rats showing near intact features.

Encapsulation of A. stipularis shoots extract into PLGA nanoparticles

As shown in Figure 5, the DLS data indicated that the mean particle size of the unloaded NPs was about 244 ± 4 nm with a PdI of 0.11 ± 0.02, and a ZP of about −21.3 ± 3.1 mV. ASD-loaded NPs had an average hydrodynamic diameter of about 248 ± 5 nm, a PdI of 0.13 ± 0.01, and a ZP of −24.7 ± 1.3 mV (Figure 6). In addition, the SEM analysis showed the spherical shape and smooth surface of NPs confirm the uniform size distribution (Figure 7). The obtained NPs showed an EE of 75.5 ± 3.2%.

Fourier-transform infrared spectroscopy analysis

A major goal in preparing NPs is to fully load the carrier with the drug. Therefore, addressing this topic is particularly important. For this target, ATR-FTIR spectra of ASD, physical mixture, PLGA, unloaded NPs, and the ASD-loaded NPs were performed after freeze-drying, as shown in Figure 8. The results of ASD showed a peak at 3253 cm^{-1}, attributed to the stretching of the hydroxyl groups of carbohydrate and water and to the N–H stretching of proteins. The peak at 2928 cm^{-1} is due to asymmetrical CH_2 groups of lipids stretching. The peak at 1400 cm^{-1} is due to the CH_3 asymmetric deformation. The ATR-FTIR spectrum of the extract revealed peaks of absorptions at 1227 and 1044 cm^{-1}. This region represents the fingerprint of polysaccharides. The infrared spectrum of the PLGA shows the characteristic absorption peak at 1744 cm^{-1} assigned to the ester group.

Differential scanning calorimetry analysis

DSC analysis is a powerful technique that provides information on physical properties such as crystalline or amorphous nature of samples. The DSC thermogram of PLGA, ASD extract as well as PLGA-ASD NPs was analyzed. PLGA exhibits a glass transition temperature at 51 °C (Figure 9(a)). No significant melting point was observed in PLGA, due to its amorphous nature. The thermogram of the extract of *A. stipularis* gives rise to a peak at 141 °C corresponding to the melting point of the crystalline regions (Figure 9(b)). To study the effect of the encapsulation of the extract on its thermal properties, DSC analyses were performed on the PLGA/extract formulation (ASD-PLGA) (Figure 9(c)).

Discussion

Alpha-amylase is a key enzyme responsible for the digestion of carbohydrates. One of the main therapeutic strategies for lowering postprandial hyperglycemia is to inhibit carbohydrate-hydrolyzing enzymes, such as α-amylase, in the intestine [24]. In the present study, ASD administration to HFrD-fed rats significantly reduced serum α-amylase activity, similar to the effect of metformin. Previous LC–MS analysis of ASD identified phenolic acids and flavonoids as major constituents [13], which have been reported to exhibit strong binding affinity toward salivary α-amylase [25,26]. Pancreatic lipase catalyzes the hydrolysis of dietary fats and phospholipids and participates in the metabolic processing of lipoproteins such as LDL and HDL cholesterol [27]. Therefore, pancreatic lipase inhibitors are among the most prescribed agents for obesity management. Our results demonstrated a significant reduction in serum lipase activity in both HFrD + ASD(H)

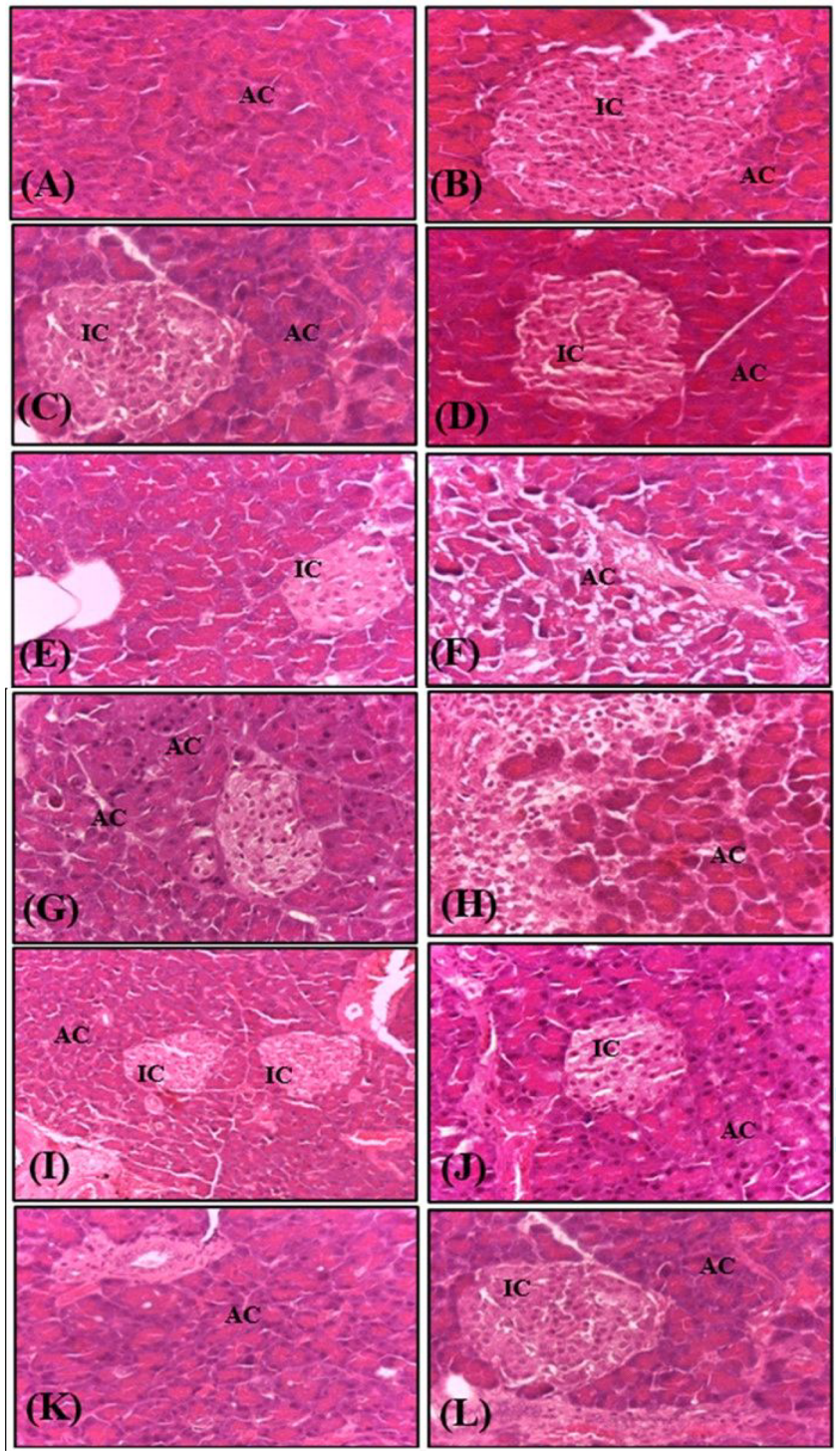

Figure 4. Photomicrographs of pancreas sections: (A, B, ×40) Control group showing normal architecture of pancreas with lobular arrangement of acini with islets of Langerhans. (C, D, ×40) Pancreas of normal rats fed ASD 100 and 300 mg/kg, respectively, the pancreas shows normal appearance. (E, F, ×40) Pancreas of rats fed HFrD, the pancreas showed atrophy in the islets of Langerhans cells (E, ×40), lymphocytic infiltration and fibrosis (F, ×40). (G, H, ×40) Pancreas of rats fed HFrD + metformin (150 mg/kg) showing a partial regeneration of its architecture. (I, ×10, J, ×40) Pancreas of rats fed HFrD + ASD (100 mg/kg), showing atrophy in the islets of Langerhans cells (I, ×10) although some regeneration is visible. (K, L, ×40) Pancreas of rats fed HFrD + ASD (300 mg/kg), showing nearly normal architecture of pancreas. AC: acinar cells; IC: islet cells.

and HFrD + ASD(L) groups. The use of lipase inhibitors derived from natural products has been considered an effective strategy against obesity, as several plant and fruit extracts have been reported to inhibit pancreatic lipase [28,29]. Phenolic compounds such as *p*-hydroxybenzoic acid, quercetin, and kaempferol,

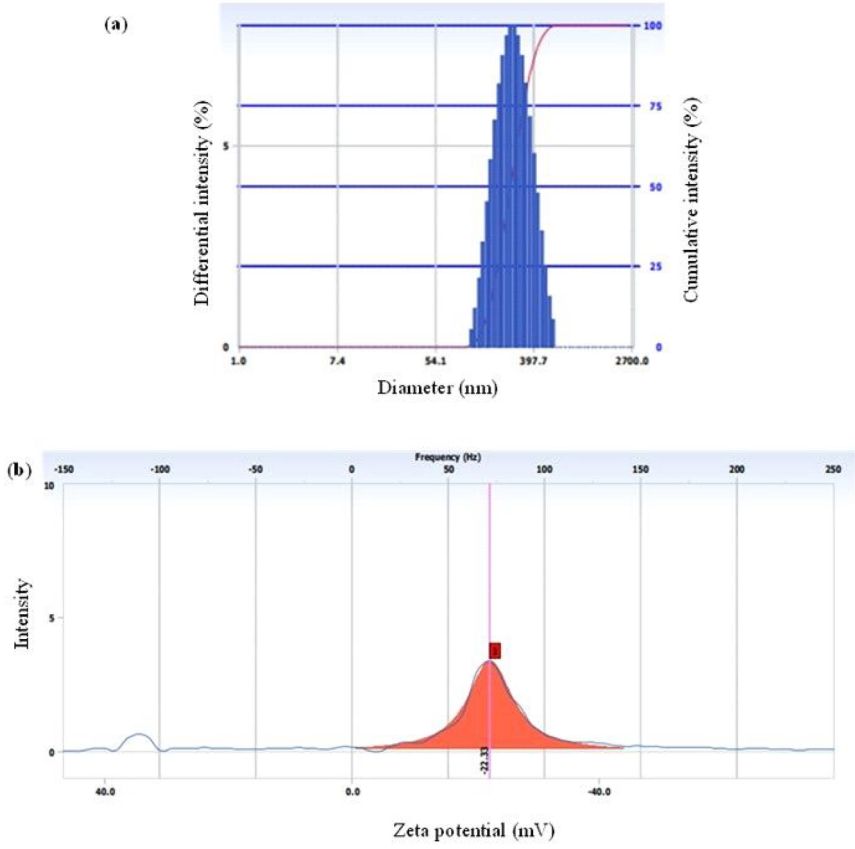

Figure 5. DLS analysis of the blank NPs: (a) average particle size and (b) zeta potential graphs.

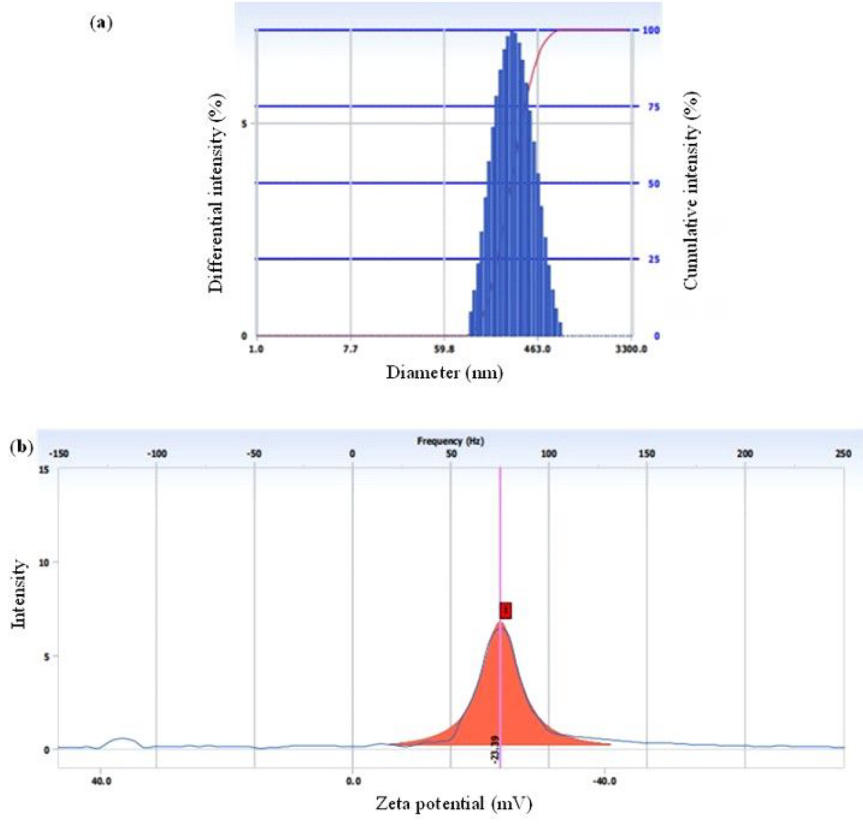

Figure 6. DLS analysis of the ASD-NPs: (a) average particle size and (b) zeta potential graphs.

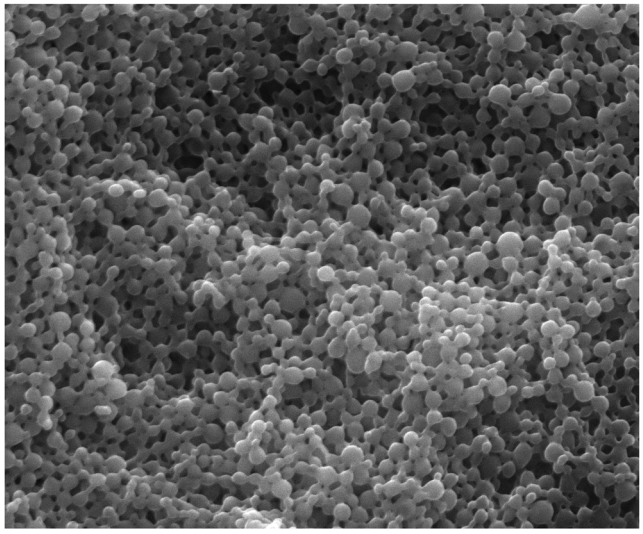

Figure 7. SEM image of the ASD-loaded PLGA nanoparticles.

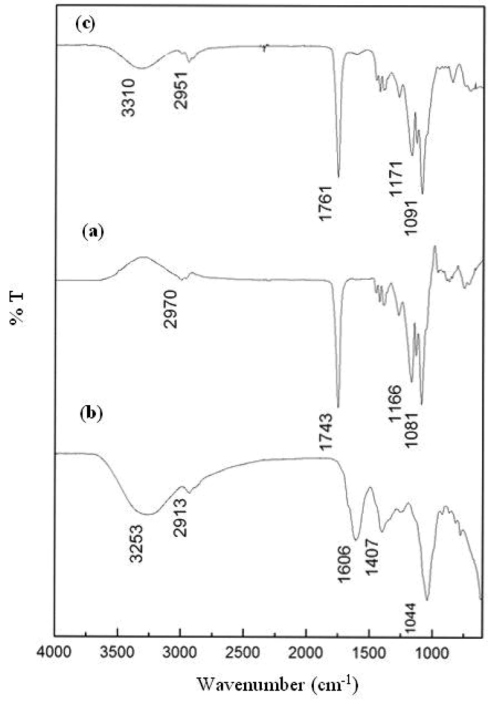

Figure 8. FTIR spectra of (a) PLGA, (b) ASD, and (c) ASD-loaded PLGA nanoparticles.

which are present in ASD [13], have also been recognized as potent lipase inhibitors [26,30].

Increased LP disrupts membrane function by decreasing membrane fluidity and altering the activity of membrane-bound enzymes and receptors [31]. Studies have shown that fructose consumption induces metabolic abnormalities in the liver, heart, kidney, and pancreas, leading to oxidative stress [4,32]. Fructose-induced insulin resistance elevates glucose oxidation and promotes the formation of reactive hydroxyl radicals [33]. In this study, ASD supplementation prevented LP in a dose-dependent manner. Similar protective effects against oxidative membrane damage have been reported for various *Asparagus* species [34,35]. These effects are likely attributed to phenolic compounds, particularly quercetin and gallic acid, which act as reductants by donating electrons to stabilize free radicals and terminate chain reactions [36,37]. Additionally, flavonols such as quercetin have been reported to inhibit xanthine oxidase and lipoxygenase [38,39].

Our findings regarding the enzymatic antioxidants CAT, SOD, and GPx in pancreatic tissues are in agreement with earlier studies [40,41] showing a marked decrease in antioxidant enzyme activity in fructose-fed rats. The current results align with literature describing the antioxidant benefits of *Asparagus* species. For instance, *A. racemosus* root extract was shown to enhance hepatic antioxidant status (SOD, CAT, and ascorbic acid) in hypercholesterolemic rats [42,43], whereas *A. cochinchinensis* aqueous extract improved antioxidant enzyme expression and nitric oxide levels [44,45]. Previous research demonstrated that metformin treatment in high-fat-fed rats enhances antioxidant defenses by partially inhibiting mitochondrial complex I, thereby reducing reactive oxygen species (ROS) generation [46]. Accordingly, the antioxidant potential of ASD may be one of the mechanisms through which this extract improves pancreatic oxidative balance. Polyphenols have been shown to mitigate oxidative stress by directly scavenging ROS or by stimulating endogenous antioxidant defenses [47]. Moreover, natural antioxidants such as phenolic acids and flavonoids can induce CAT and SOD gene transcription through activation of nuclear factor erythroid 2-related factor 2 (Nrf2), a master regulator of the

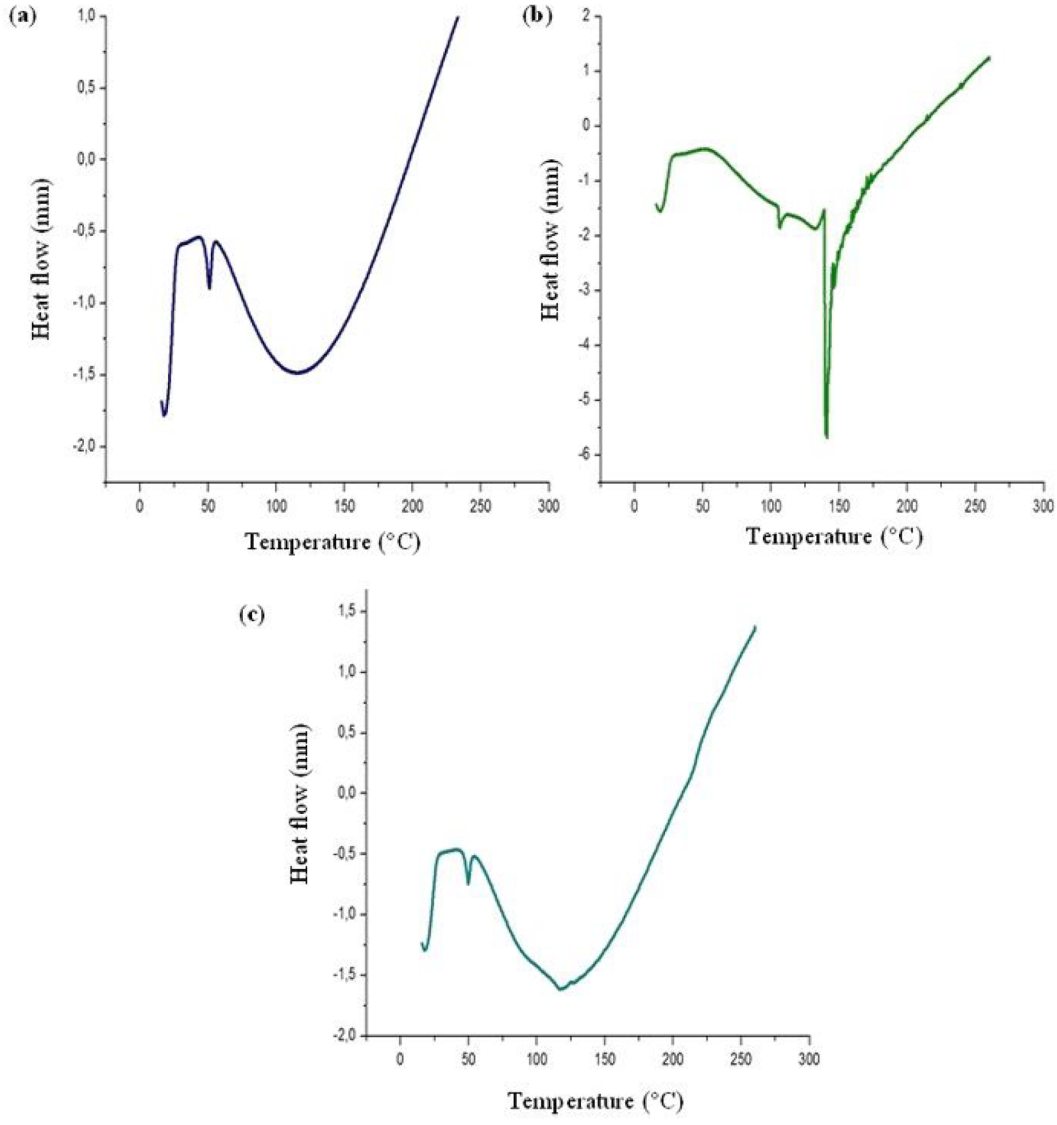

Figure 9. DSC thermogram of (a) PLGA, (b) ASD, and (c) ASD-loaded PLGA nanoparticles.

antioxidant response [48,49]. Activation of Nrf2 has been associated with enhanced antioxidant recruitment and is considered a promising therapeutic target in diabetes management [50].

Antioxidants are widely recognized as effective therapeutic agents against oxidative-stress-induced pancreatic injury, owing to their ability to neutralize ROS, enhance endogenous antioxidant systems, and protect pancreatic β-cell integrity [51,52]. The protective mechanism of ASD may thus be linked to its antioxidant capacity, reflected in the activities of GPx, SOD, MDA, and CAT. ASD shoots have been shown to contain several phenolic acids and flavonoids [13] which stimulate antioxidant enzyme gene expression and decrease MDA levels [38,39,47]. These findings support that antioxidants in *A. stipularis* extracts may confer protection against pancreatic damage induced by HFrD, consistent with our histopathological observations. Nevertheless, since metabolic syndrome in humans is a multifactorial pathology, further studies will be required to fully unveil the mechanistic effects of ASD, as well as its pharmacokinetic profile.

The functional properties of NPs – such as drug release, cellular uptake, *in vivo* biodistribution, and stability – are largely influenced by particle size, PdI, and ZP [53,54]. When comparing the similar results for unloaded and ASD NPs, it was verified that the production method allowed to obtain NPs with a small size, narrow size distributions, and good colloidal stability [54]. Hill et al. [55] encapsulated cinnamon root extract using biodegradable PLGA (ratios 65:35 and 50:50), obtaining NPs of 145–167 nm in diameter with encapsulation efficiencies of 39% and 48%, respectively. Likewise, Pereira et al. [56] prepared PLGA NPs containing carotenoid-rich extract from *Campomanesia xanthocarpa* fruit, achieving spherical particles (145–162 nm) with

high encapsulation efficiencies (83.7% and 98.5%). More recently, Mendez-Pfeiffer et al. [57] developed *Sonoran propolis*-loaded PLGA NPs exhibiting an average ZP of −21.2 ± 0.7 mV, mean size 152.6 ± 7.1 nm, and EE ≈ 68%. The study of the FTIR spectrum of the NP (PLGA/extract) aims to show possible shift in the location of certain absorption peaks, and the appearance or disappearance of new peaks in comparison to the polymer or extract alone. The results showed that during the preparation of PLGA NPs, the characteristic peak of PLGA was not modified. This suggests that there was no chemical interaction between the functional groups of the extract and the polymer during encapsulation process. For the DSC analysis, we noticed the absence of the peak corresponding to the melting point of the crystalline regions of the extract. This suggests a lack of crystallinity and an amorphous structure for the extract loaded into NPs. This proof-of-concept displays the suitability to encapsulate ASD into a nanoformulation, opening the door for its potential application in food supplementation and nutraceuticals. Future endeavors will include detailed evaluation of this nanoformulation *in vitro* and *in vivo*, to further assess the impact of ASD-loaded NPs in metabolic syndrome, including detailed mechanistic, safety, stability, reproducibility, and pharmacokinetic studies.

Conclusion

The present study reveals that *A. stipularis* extract has potent antioxidative and β-cell protection activities in HFrD induced metabolic syndrome in rats, based on its ability to decrease α-amylase and pancreatic lipase activities. These findings also suggests that the antioxidant properties exhibited by ASD can contribute for the scientific reasoning for the folk medicine application of this natural matrix, namely for the treatment of diabetes and dyslipidemias. For the first time, the formulation of spherical PLGA NPs loaded with an aqueous extract of *A. stipularis* using the solvent evaporation approach has been demonstrated in the current work, with great efficiency, opening the door for the future application of this nutraceutical formulation in therapeutics and/or food supplementation, using different routes of administration. Future endeavors in this field will include the evaluation of the bioactivity and effectiveness of the newly developed ASD-loaded NPs.

Acknowledgements

We thank to ALIES, for the international fellowship in Natural Bioactives Lab awarded to Khaoula Adouni.

Author contributions

CRediT: **Khaoula Adouni**: Investigation, Methodology, Writing – original draft; **Olfa Zouaoui**: Formal analysis, Investigation; **Pedro Brandão**: Validation, Writing – review & editing; **Patrícia Rijo**: Conceptualization, Methodology; **Sofia A. Costa Lima**: Methodology, Writing – review & editing; **Salette Reis**: Resources, Writing – review & editing; **Lotfi Achour**: Supervision, Validation; **Pedro Fonte**: Funding acquisition, Resources, Supervision.

Disclosure statement

The authors confirm that they have no conflicts of interest with respect to the work described in this manuscript. P. Fonte is an Associate Editor of this journal.

Funding

This work was funded by Fundação para a Ciência e a Tecnologia (FCT), Portugal in the scope of the projects UID/04326/2025 (DOI https://doi.org/10.54499/UID/04326/2025), UID/PRR/04326/2025 (DOI https://doi.org/10.54499/UID/PRR/04326/2025), and LA/P/0101/2020 (DOI:10.54499/LA/P/0101/2020) of the Research Unit Center for Marine Sciences – CCMAR; UID/04565/2025 of the Research Unit Institute for Bioengineering and Biosciences – iBB, and LA/P/0140/2020 of the Associate Laboratory Institute for Health and Bioeconomy – i4HB; and the project UIDB/04585/2020 (DOI: 10.54499/UIDB/04585/2020) of the Research Unit CiiEM.

Data Availability Statement

The data that support the findings of this study are available from the corresponding author upon reasonable request.

References

[1] International Diabetes Federation. IDF Diabetes Atlas. 11th ed. Brussels: IDF; 2025.
[2] World Health Organization. Diabetes fact sheet. Geneva: WHO; 2022.
[3] Hannou SA, Haslam DE, McKeown NM, et al. Fructose metabolism and metabolic disease. J Clin Invest. 2018;128(2):545–555. doi: 10.1172/JCI96702.
[4] Li Z, Fan X, Gao F, et al. Fructose metabolism and its roles in metabolic diseases, inflammatory diseases, and cancer. Mol Biomed. 2025;6(1):43. doi: 10.1186/s43556-025-00287-2.
[5] Baumann A, Brandt A, Bergheim I. Fructose, a trigger of metabolic diseases? A narrative review. Explor Dig Dis. 2022;1:51–71. doi: 10.37349/edd.2022.00005.
[6] Wu Y, Wong CW, Chiles EN, et al. Glycerate from intestinal fructose metabolism induces islet cell damage and glucose intolerance. Cell Metab. 2022;34(7):1042–1053. e6. doi: 10.1016/j.cmet.2022.05.007.

[7] Mvelase Z, Luvuno M, Mabandla MV. Influence of high fructose intake on systemic and cognitive health across developmental stages: a review. Endocr Metab Sci. 2025;19:100256. doi: 10.1016/j.endmts.2025.100256.
[8] Horváth L, Novodvorský P, Haluzík M. Practical limitations of complex insulin therapies in type 2 diabetes: focus on therapy simplification using fixed-ratio combinations of basal insulin and a glucagon-like peptide-1 receptor agonist. Diabetes Obes Metab. 2025;27(Suppl. 7):42–54. doi: 10.1111/dom.16645.
[9] Wu J, Sahoo JK, Li Y, et al. Challenges in delivering therapeutic peptides and proteins: a silk-based solution. J Control Release. 2022;345:176–189. doi: 10.1016/j.jconrel.2022.02.011.
[10] Salleh NH, Zulkipli IN, Yasin HM, et al. Systematic review of medicinal plants used for treatment of diabetes in human clinical trials: an ASEAN perspective. Evid Based Complement Alternat Med. 2021;2021:5570939. doi: 10.1155/2021/5570939.
[11] Deora N, Venkataraman K. A systematic review of medicinal plants and compounds for restoring pancreatic β-cell mass and function in the management of diabetes mellitus. J Appl Pharm Sci. 2023;13(7):55–72. doi: 10.7324/JAPS.2023.130422.
[12] Uti DE, Atangwho IJ, Alum EU, et al. Natural antidiabetic agents: current evidence and development pathways from medicinal plants to clinical use. Nat Prod Commun. 2025;20(3):1–29. doi: 10.1177/1934578X251323393.
[13] Adouni K, Zouaoui O, Chahdoura H, et al. In vitro antioxidant activity, α-glucosidase inhibitory potential and in vivo protective effect of *Asparagus stipularis* Forssk. aqueous extract against high-fructose diet-induced metabolic syndrome in rats. J Funct Foods. 2018;47:521–530. doi: 10.1016/j.jff.2018.06.006.
[14] Marecki EK, Oh KW, Knight PR, et al. Poly(lactic-co-glycolic acid) nanoparticle fabrication, functionalization, and biological considerations for drug delivery. Biomicrofluidics. 2024;18(5):051503. doi: 10.1063/5.0201465.
[15] Shakya AK, Al-Sulaibi M, Naik RR, et al. Review on PLGA polymer-based nanoparticles with antimicrobial properties and their application in various medical conditions or infections. Polymers. 2023;15(17):3597. doi: 10.3390/polym15173597.
[16] Naz S, Khurshid A, Hassan SMU, et al. *Fagonia indica* extract encapsulated in PLGA nanocarriers demonstrated enhanced therapeutic efficacy through improved intracellular uptake of photoactive metabolites. Sci Rep. 2025;15(1):23140. doi: 10.1038/s41598-025-50503-3.
[17] Bradford MM. A rapid and sensitive method for the quantitation of microgram quantities of protein utilizing the principle of protein–dye binding. Anal Biochem. 1976;72(1–2):248–254. doi: 10.1016/0003-2697(76)90527-3.
[18] Nasri R, Abdelhedi O, Jemil I, et al. Preventive effect of goby fish protein hydrolysates on high-fat–high-fructose diet-induced hyperglycemia, oxidative stress, and deterioration of kidney function in rats. Food Funct. 2015;6(10):3259–3270.
[19] Aguilar Diaz De Leon J, Borges CR. Evaluation of oxidative stress in biological samples using the thiobarbituric acid reactive substances assay. J Vis Exp. 2020;159:e61122. doi: 10.3791/61122.
[20] Histo Flohé L, Günzler WA. Assays of glutathione peroxidase. Methods Enzymol. 1984;105:114–121.
[21] Nezelof C, Gollé L. Fixation et étude histologique du pancréas humain et expérimental. Arch Anat Pathol. 1972;20(2):141–160.
[22] Fonte P, Soares S, Sousa F, et al. Stability study perspective of the effect of freeze-drying using cryoprotectants on the structure of insulin loaded into PLGA nanoparticles. Biomacromolecules. 2014;15(10):3753–3765. doi: 10.1021/bm5010383.
[23] Adouni K, Júlio A, Santos-Buelga C, et al. Roots and rhizomes of wild *Asparagus*: nutritional composition, bioactivity, and nanoencapsulation of the most potent extract. Food Biosci. 2022;45:101334. doi: 10.1016/j.fbio.2021.101334.
[24] Ullah H, Uddin I, Ali HZ, et al. A promising α-glucosidase and α-amylase inhibitors based on benzimidazole–oxadiazole hybrid analogues: evidence based in vitro and in silico studies. Results Chem. 2024;11(2):101832. doi: 10.1016/j.rechem.2024.101832.
[25] Kulkarni S, Dwivedi P, Danappanvar AN, et al. Identification of α-amylase inhibitors from flavonoid fraction of *Feronia elephantum* and its integration with in-silico studies. In Silico Pharmacol. 2021;9(1):50. doi: 10.1007/s40203-021-00099-6.
[26] Martinez-Gonzalez AI, Díaz-Sánchez ÁG, de la Rosa LA, et al. Inhibition of α-amylase by flavonoids: structure–activity relationship (SAR). Spectrochim Acta A Mol Biomol Spectrosc. 2019;206:437–447. doi: 10.1016/j.saa.2018.08.080.
[27] Subramaniyan V, Hanim YU. Role of pancreatic lipase inhibition in obesity treatment: mechanisms and challenges towards current insights and future directions. Int J Obes. 2025;49(3):492–506. doi: 10.1038/s41366-024-01675-z.
[28] Birari RB, Bhutani KK. Pancreatic lipase inhibitors from natural sources: unexplored potential. Drug Discov Today. 2007;12(19–20):879–889. doi: 10.1016/j.drudis.2007.07.024.
[29] McDougall GJ, Kulkarni NN, Stewart D. Berry polyphenols inhibit pancreatic lipase in vitro. Food Chem. 2009;115(1):193–199. doi: 10.1016/j.foodchem.2008.11.093.
[30] Li M-M, Chen Y-T, Ruan J-C, et al. Structure–activity relationship of dietary flavonoids on pancreatic lipase. Curr Res Food Sci. 2023;6:100424. doi: 10.1016/j.crfs.2022.100424.
[31] Ayala A, Muñoz MF, Argüelles S. Lipid peroxidation: production, metabolism, and signaling mechanisms of malondialdehyde and 4-hydroxy-2-nonenal. Oxid Med Cell Longev. 2014;2014:360438. doi: 10.1155/2014/360438.
[32] Jegatheesan P, De Bandt JP. Fructose and NAFLD: the multifaceted aspects of fructose metabolism. Nutrients. 2017;9(3):230. doi: 10.3390/nu9030230.
[33] Herman MA, Birnbaum MJ. Molecular aspects of fructose metabolism and metabolic disease. Cell Metab. 2021;33(12):2329–2354. doi: 10.1016/j.cmet.2021.09.010.
[34] Taepongsorat L, Phadungkit M. Effects of *Asparagus racemosus* root extracts on serum lipid profiles, lipid peroxidation and superoxide dismutase in ovariectomized rats. PJ. 2018;10(5):1036–1041. doi: 10.5530/pj.2018.5.175.
[35] Vázquez-Castilla S, De la Puerta R, Garcia-Gimenez MD, et al. Bioactive constituents from "Triguero" asparagus

improve the plasma lipid profile and liver antioxidant status in hypercholesterolemic rats. Int J Mol Sci. 2013;14(11):21227–21239. doi: 10.3390/ijms141121227.

[36] Singh DP, Verma S, Prabha R. Investigations on antioxidant potential of phenolic acids and flavonoids: common phytochemical ingredients in plants. J Plant Biochem Physiol. 2018;6(3):219. doi: 10.4172/2329-9029.1000219.

[37] Platzer M, Kiese S, Tybussek T, et al. Radical scavenging mechanisms of phenolic compounds: a quantitative structure–property relationship (QSPR) study. Front Nutr. 2022;9:882458. doi: 10.3389/fnut.2022.882458.

[38] Sadik CD, Sies H, Schewe T. Inhibition of 15-lipoxygenase by flavonoids: structure–activity relationship and mechanism. Biochem Pharmacol. 2003;65(5):773–781. doi: 10.1016/s0006-2952(02)01522-4.

[39] Xue H, Xu M, Gong D, et al. Mechanism of flavonoids inhibiting xanthine oxidase and alleviating hyperuricemia from structure–activity relationship and animal experiments: a review. Food Front. 2023;4(4):1643–1665. doi: 10.1002/fft2.287.

[40] Mirzaei R, Khosrokhavar R, Arbabi Bidgoli S. The role of high-fructose diet in liver function of rodent models: a systematic review of molecular analysis. Iran Biomed J. 2023;27(6):326–339. doi: 10.52547/ibj.3965.

[41] Güney C, Akar F. The possible mechanisms of high-fructose diet-induced pancreatic disturbances. J Res Pharm. 2023;27(2):753–761. doi: 10.29228/jrp.357.

[42] Visavadiya NP, Narasimhacharya AVRL. *Asparagus* root regulates cholesterol metabolism and improves antioxidant status in hypercholesteremic rats. Evid Based Complement Alternat Med. 2009;6(2):219–226. doi: 10.1093/ecam/nem091.

[43] Acharya SR, Acharya NS, Bhangale JO, et al. Antioxidant and hepatoprotective action of *Asparagus racemosus* Willd. root extracts. Indian J Exp Biol. 2012;50(11):795–801.

[44] Lei L, Ou L, Yu X. The antioxidant effect of *Asparagus cochinchinensis* (Lour.) Merr. shoot in D-galactose induced mice aging model and in vitro. J Chin Med Assoc. 2016;79(4):205–211. doi: 10.1016/j.jcma.2015.06.023.

[45] Lei L, Chen Y, Ou L, et al. Aqueous root extract of *Asparagus cochinchinensis* (Lour.) Merr. has antioxidant activity in D-galactose-induced aging mice. BMC Complement Altern Med. 2017;17(1):469. doi: 10.1186/s12906-017-1975-x.

[46] Kelly B, Tannahill GM, Murphy MP, et al. Metformin inhibits the production of reactive oxygen species from NADH: ubiquinone oxidoreductase to limit induction of interleukin-1β (IL-1β) and boosts interleukin-10 (IL-10) in lipopolysaccharide (LPS)-activated macrophages. J Biol Chem. 2015;290(33):20348–20359. doi: 10.1074/jbc.M115.662114.

[47] Rudrapal M, Khairnar SJ, Khan J, et al. Dietary polyphenols and their role in oxidative stress-induced human diseases: insights into protective effects, antioxidant potentials and mechanism(s) of action. Front Pharmacol. 2022;13:806470. doi: 10.3389/fphar.2022.806470.

[48] Martínez-Huélamo M, Rodríguez-Morató J, Boronat A, et al. Modulation of Nrf2 by olive oil and wine polyphenols and neuroprotection. Antioxidants. 2017;6(4):73. doi: 10.3390/antiox6040073.

[49] Mendonca P, Soliman KFA. Flavonoids activation of the transcription factor Nrf2 as a hypothesis approach for the prevention and modulation of SARS-CoV-2 infection severity. Antioxidants. 2020;9(8):659. doi: 10.3390/antiox9080659.

[50] David JA, Rifkin WJ, Rabbani PS, et al. The Nrf2/Keap1/ARE pathway and oxidative stress as a therapeutic target in type II diabetes mellitus. J Diabetes Res. 2017;2017:4826724. doi: 10.1155/2017/4826724.

[51] Tang Y, Sun M, Liu Z. Phytochemicals with protective effects against acute pancreatitis: a review of recent literature. Pharm Biol. 2022;60(1):479–490. doi: 10.1080/13880209.2022.2039723.

[52] Wang J, Wang H. Oxidative stress in pancreatic beta cell regeneration. Oxid Med Cell Longev. 2017;2017(1):1930261. doi: 10.1155/2017/1930261.

[53] Danaei M, Dehghankhold M, Ataei S, et al. Impact of particle size and polydispersity index on the clinical applications of lipidic nanocarrier systems. Pharmaceutics. 2018;10(2):57. doi: 10.3390/pharmaceutics10020057.

[54] Kaplan M, Öztürk K, Öztürk SC, et al. Effects of particle geometry for PLGA-based nanoparticles: preparation and in vitro/in vivo evaluation. Pharmaceutics. 2023;15(1):175. doi: 10.3390/pharmaceutics15010175.

[55] Hill LE, Taylor TM, Gomes C. Antimicrobial efficacy of poly(DL-lactide-co-glycolide) (PLGA) nanoparticles with entrapped cinnamon bark extract against *Listeria monocytogenes* and *Salmonella typhimurium*. J Food Sci. 2013;78(4):N626–N632. doi: 10.1111/1750-3841.12069.

[56] Pereira MC, Hill LE, Zambiazi RC, et al. Nanoencapsulation of hydrophobic phytochemicals using poly(DL-lactide-co-glycolide) (PLGA) for antioxidant and antimicrobial delivery applications: guabiroba fruit (*Campomanesia xanthocarpa* O. Berg) study. LWT Food Sci Technol. 2015;63(1):100–107. doi: 10.1016/j.lwt.2015.03.062.

[57] Mendez-Pfeiffer P, Juarez J, Hernandez J, et al. Polymeric nanoparticles for the delivery of Sonoran desert propolis: synthesis, characterization and antiproliferative activity on cancer cells. Colloids Surf B Biointerfaces. 2022;215:112475. doi: 10.1016/j.colsurfb.2022.112475.